JOURNAL OF VIROLOGY, June 1993, p. 3295–3303
0022-538X/93/063295-09$02.00/0

Vol. 67, No. 6

Contributions of the Brome Mosaic Virus RNA-3 3′-Nontranslated Region to Replication and Translation

FREDERICK C. LAHSER, LOREN E. MARSH,† AND TIMOTHY C. HALL*

Institute of Developmental and Molecular Biology and Department of Biology, Texas A&M University, College Station, Texas 77843-3155

Received 2 February 1993/Accepted 8 March 1993

Sequences upstream of the 3′-terminal tRNA-like structure of brome mosaic virus RNAs have been predicted to fold into several stem-loop and pseudoknot structures. To elucidate the functional role of this upstream region, a series of deletions was made in cDNA clones of RNA-3, a genomic component not required for replication. These deletion mutants were transcribed in vitro and cotransfected with RNA-1 and RNA-2 into barley protoplasts. Deletion of single stem-loop structures gave progeny retaining near-wild-type accumulation levels. Constructions representing deletion of two or three stem-loops substantially lowered the accumulation of progeny RNA-3 relative to wild-type levels. RNA-3 mutants bearing deletions of longer sequences or of the entire region (ΔPsKs RNA-3) replicated poorly, yielding no detectable RNA-3 or RNA-4 progeny. Levels of RNA-1 and RNA-2, in the presence of a mutant RNA-3, were found to increase relative to the accumulation observed in a complete wild-type transfection. The stability of ΔPsKs RNA-3 in protoplasts was somewhat lower than that of wild-type RNA during the first 3 h postinoculation. Little difference in translatability in vitro of wild-type and RNA-3 constructs bearing deletions within the stem-loop region was observed, and Western immunoblot analysis of viral coat protein produced in transfected protoplasts showed that protein accumulation paralleled the amount of RNA-4 message produced from the various sequences evaluated. These results indicate that the RNA-3 pseudoknot region plays a minor role in translational control but contributes substantially to the overall replication of the brome mosaic virus genome.

Brome mosaic virus (BMV), which infects many monocot plants, possesses a single-stranded positive-sense tripartite genome. The 3′ 200 nucleotides of the three genomic and single subgenomic RNAs are similar in sequence and secondary structure (3). This region has been shown to be multifunctional, containing the minimal negative-strand promoter (10, 38) and recognition sites for host nucleotidyltransferase (38, 47) and tyrosine synthetase (11, 24).

The organization of the terminal 134 nucleotides is tRNA-like, the tyrosine acceptor stem being formed by a pseudoknot (28, 49). Pseudoknots are RNA stem-loop structures that typically possess base complementarity between the loop and adjacent sequences (41), although long-distance (~900 nucleotides) interactions can be involved, as in the predicted secondary structure of 16S rRNA of *Escherichia coli* (54). Since the 3′ valine-accepting helical stem of turnip yellow mosaic virus (TYMV) RNA was shown to be formed by a pseudoknot (50), this motif has been found in several functional RNA structures, including sites for recognition of translational repressors (57) and ribosomal frameshifting (25, 52, 58). Studies of the 3′-nontranslated region (3′-NTR) of tobacco mosaic virus (TMV) RNA have provided evidence for five pseudoknots, two in the tRNA-like structure (48) and three in the adjacent upstream region (59). The 3′-NTR of BMV RNA-3 is predicted (42, 43) to have five pseudoknots, four being upstream of the tRNA-like structure; additionally, there are three nonpseudoknotted stem-loop structures in this upstream region (Fig. 1A).

Only two reports (19, 56), both for TMV RNA, have to date addressed the role of upstream pseudoknot structures in viral RNAs. Takamatsu et al. (56) found that deletion of the central pseudoknot debilitated systemic spread, while deletion or destabilization of the 3′ proximal structure drastically reduced RNA replication. Gallie and Walbot (19) used a reporter gene, the β-glucuronidase (GUS) gene, to analyze the contribution of the TMV RNA 3′-NTR to message stability and translatability. They concluded that the 3′-NTRs, and in particular the sequences forming upstream pseudoknots, of aminoacylatable plant viral RNA genomes perform a stabilizing role, since the half-life of a GUS-TMV 3′-NTR chimera was found to be effectively analogous to that of a GUS-poly(A) mRNA. Although an enhancement in the translatability of chimeric GUS mRNAs bearing the 3′-NTR of TMV RNA was attributed to the pseudoknot-containing sequences (19), a subsequent study (18) suggested that the degree to which a downstream sequence contributes to translation is modulated by the reporter gene used in the analysis.

In this study, the role of this untranslated stem-loop region in the replication of BMV has been assessed by measuring the relative amounts of progeny RNA obtained when RNA-3 mutants bearing sequence deletions within this region were cotransfected into barley protoplasts with wild-type (wt) RNA-1 and -2. The reduced efficacy of the negative-strand promoter found for these RNA-3 deletion mutants suggests that a correct spatial context is required for initiation of replication. Additionally, to learn whether the 3′-NTR of RNA-3 fulfills the functional role of a poly(A) tail in the natural context of the viral sequence, the input stability in protoplasts and translatability in vitro of these mutant RNAs were also studied. Since some mutations were observed to negatively affect the yield of subgenomic RNA-4 in vivo, coat protein production was also assayed. The presence of this sequence in the 3′-NTR of BMV, and the potential secondary structures that it forms, may play only a second-

* Corresponding author. Electronic mail (INTERNET) address: tim@bio.tamu.edu

† Present address: Department of Plant Pathology, Cornell University, Ithaca, NY 14853.

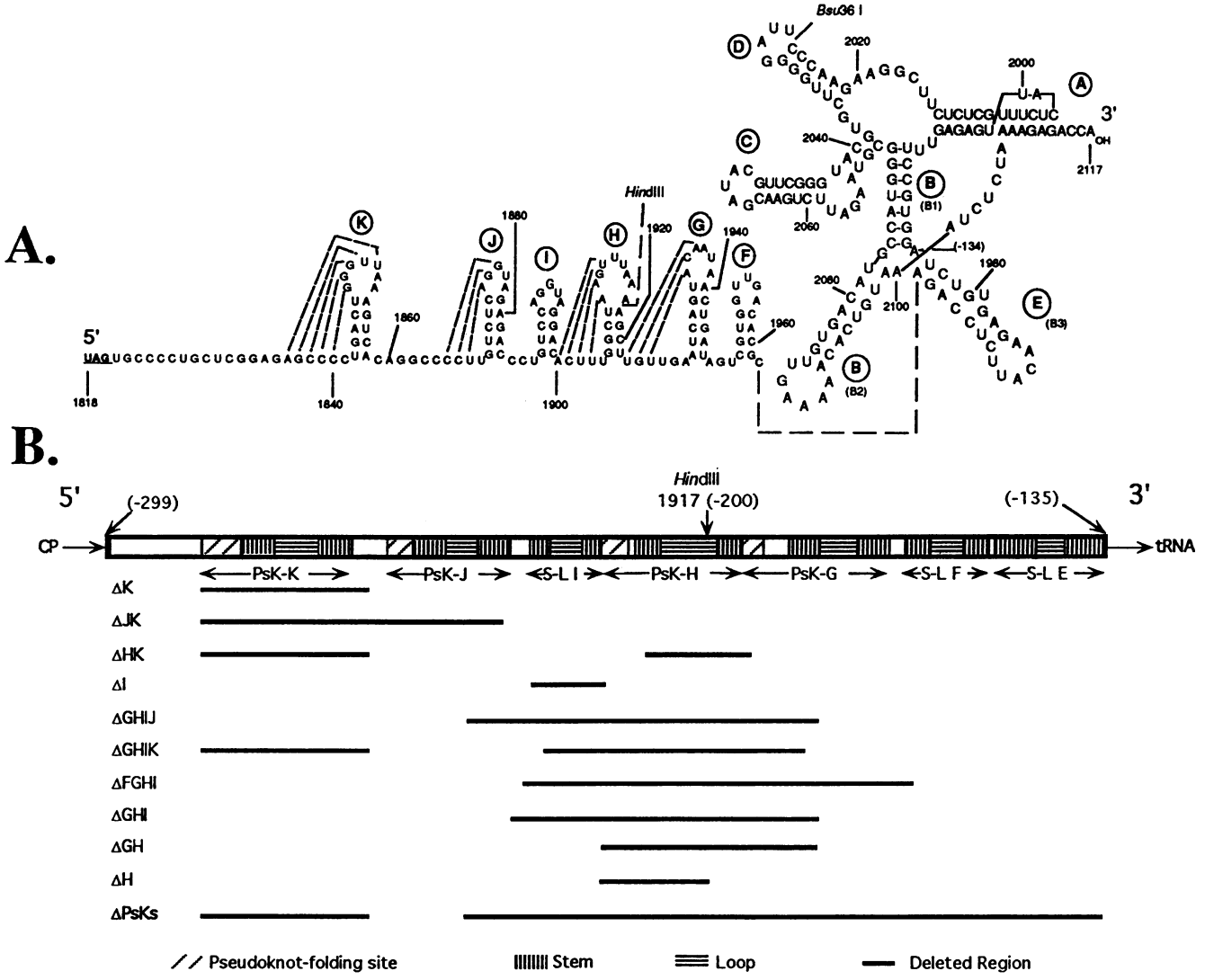

FIG. 1. Diagram of the 3′-NTR of BMV RNA-3 and deletion map. Nucleotide positions from the 5′ end of genomic RNA-3 are indicated, with the position from the 3′ end listed in parentheses as a negative number. The positions of a unique *Hin*dIII restriction site (base 1917), used in previous studies (10–13) and a unique *Bsu*36I restriction site (base 2026) in the cDNA are indicated. The stem-loop structures (A to K) are named in accordance with their position from the 3′ terminus. (A) Sequence and predicted secondary structure (42, 43). Stems A to E, which compose the tRNA-like structure, are arranged on the basis of synthetase protection studies by Perret et al. (40), from which the nomenclature (B1 to B3) was used. The position of the 134th nucleotide from the 3′ end, which delimits the minimal negative-strand promoter in vitro (38), is indicated. The UAG at the 5′ end marks the stop codon for the upstream coat protein cistron. (B) Linear representation of the predicted upstream stem-loop and pseudoknot structures, following the key shown. The stop codon for the coat protein (CP) and the start of the 3′ tRNA-like structure (tRNA) are shown on the left and right ends of the linear map. The extent of a given deletion is shown as a solid bar, and the nomenclature for each mutation is based on the correlation of deleted sequence to the predicted structure(s) missing. PsK, pseudoknot structure; S-L: stem-loop.

ary role in simulating a poly(A) tail in the setting of viral RNA; the primary function of the sequences is more closely associated with replication functions.

MATERIALS AND METHODS

Chemicals and enzymes. Restriction and modifying enzymes were obtained from Boehringer-Mannheim, New England Biolabs, and Bethesda Research Laboratories. Human placental RNase inhibitor (RNA guard) and T7 RNA polymerase were from Pharmacia, and T3 RNA polymerase came from Bethesda Research Laboratories. Cap analog (m^7GpppG), mung bean nuclease, and T4 DNA ligase were from New England Biolabs. The wheat germ in vitro translation kit was obtained from Promega. All radioactive materials were purchased from New England Nuclear.

Plasmid constructs. Full-length infectious BMV RNA-1, -2, and -3 were transcribed in vitro from cDNA clones pT7B1, pT7B2, and pB3fl(+) (12, 45). Deletion of sequences corresponding to single putative structures from the RNA-3 clone were constructed by oligonucleotide site-directed mutagenesis (35, 46) of single-stranded DNA produced from the fl origin-containing pB3fl(+) plasmid. Construct ΔK RNA-3, which contains a deletion of sequences for the 5′-most pre-

dicted structure (bases 1835 to 1860; Fig. 1) and creates a unique *Apa*I site, was made by use of the oligonucleotide 5'-AGACAAGGGGCCCTCCGAGCAGGG-3'. The oligonucleotide used to delete the predicted pseudoknot structure H, 5'-TTCAACAAGCTTGTCCTACCTGGA-3', created ΔH RNA-3 (bases 1900 to 1916 deleted). Construct ΔI RNA-3, which contains a deletion of the centrally located stem-loop I (bases 1887 to 1899), was created by a third oligonucleotide, 5'-CTTAGCCAAAGTAGGGCCTCTACC-3'.

Larger deletions in the putative pseudoknot region (Fig. 1) were constructed by linearization of plasmids with either *Apa*I or *Hin*dIII and *Bal* 31 exonuclease digestion (35, 51). Deletion mutants were screened and confirmed by appropriate restriction digests and dideoxy sequencing. Mutant RNA-3 transcripts derived from these clones were ΔJK (bases 1836 to 1883 deleted), ΔHK (bases 1835 to 1860 and 1907 to 1924 deleted), ΔGH (bases 1901 to 1933 deleted), ΔGHI (bases 1884 to 1934 deleted), ΔGHIJ (bases 1878 to 1935 deleted), ΔGHIK (bases 1835 to 1860 and 1889 to 1930 deleted), ΔFGHI (bases 1885 to 1951 deleted), and ΔPsKs (bases 1835 to 1860 and 1887 to 1983 deleted). The nomenclature for the mutants was based on the correspondence of the deleted sequence to the position of a predicted structure(s). All RNA-3 mutants are predicted to maintain their respective tRNA-like structures, as well as the sequence of the minimal negative-strand promoter (38).

In vitro transcription and barley protoplast transfection. Plasmids pT7B1, pT7B2, and pB3f1(+) and its mutant derivatives were linearized with *Bam*HI and used as transcriptional templates. To transcribe an RNA lacking the tRNA-like structure without potential damage to the upstream pseudoknot or stem-loop structures, plasmid 3'Δ1984 (31), an RNA-3 deletion mutant lacking bases 1984 to 1999 of the tRNA-like structure, was linearized at a unique *Bsu*36I site (base 2026; Fig. 1), creating mutant 1984/BΔt. Capped full-length RNA transcripts were synthesized in vitro by using T7 RNA polymerase (12) and separated from the DNA template by lithium chloride precipitation (47). Barley (*Hordeum vulgare* cv. Dickson) protoplasts were isolated (33) and inoculated by the polyethylene glycol method (12). Approximately 2.5×10^5 protoplasts were inoculated with 1 μg of each RNA component and incubated at room temperature under fluorescent lights for 24 h. To monitor the stability of inoculum RNA, 3 μg of a selected RNA-3 transcript was transfected into approximately 10^6 protoplasts, divided into four equal aliquots, and harvested at 0-, 3-, 6-, and 12-h time points. RNA was extracted with sodium dodecyl sulfate (SDS) and phenol-chloroform and then precipitated with ethanol (33).

Analysis of progeny and inoculum RNA from protoplasts. Total RNA samples from infected protoplasts were equally divided and analyzed by Northern (RNA) hybridizations (12). Highly specific positive- and negative-sense ^{32}P-labeled RNA probes were transcribed from plasmid pT73TR, using either T3 or T7 RNA polymerase (47). This plasmid contains the cDNA corresponding to the tRNA-like structure (3'-terminal 200 bp), which is conserved among all BMV RNAs. The use of probes of equal length and specific activity permitted direct molar comparison of positive- and negative-strand viral RNA levels. To measure the amount of input RNA-3 transcripts in stability assays, RNA-3-specific probes corresponding to bases 601 to 1221 were used to detect positive-sense RNA-3. Levels of progeny positive- and negative-strand viral RNAs and of remaining input RNA-3 transcripts were measured by video densitometry from preflashed Northern autoradiographs (32). The level of each BMV RNA component in a replication assay is expressed as a percentage of the total viral RNA in a protoplast infection. These values were compared with their counterparts in a parallel wt infection and are expressed in the text as a relative percent difference. Levels of residual RNA-3 in stability assays are reported as a percentage of the RNA at a given time point in relation to the amount measured at the zero time point, normalized to represent 100% of the protoplast inoculum. Results from both assays were based on averages from at least two independent experiments.

Analysis of protein production from wt and mutant RNA-3 transcripts in vitro and in vivo. Translation in a wheat germ in vitro system was performed according to the manufacturer (Promega), with the following modifications. In a 25-μl reaction, limiting amounts (0.5 μg) of an RNA-3 transcript were heated in water for 5 min at 65°C and then quenched on ice prior to the addition of the remaining reaction components. Final reaction conditions included 100 mM potassium acetate and 0.2 mCi of [^{35}S]methionine (1,140 Ci/mmol) per ml. Reaction mixtures were incubated at 30°C, and 4-μl aliquots were spotted onto 20% trichloroacetic acid-soaked paper filters at 0-, 10-, 20-, and 40-min time points. Incorporation of [^{35}S]methionine was determined by counting trichloroacetic acid-precipitable material on filter paper disks (37). The rate of incorporation in a reaction was determined, and the percentage of total label incorporated into protein for each mutant messenger was calculated and normalized to the level obtained in the presence of wt RNA-3. Averages were based on at least two independent experiments.

To assess relative translation levels of the mutant sequences in vivo, Western immunoblot analyses of viral coat protein produced in protoplasts transfected with RNA-1 plus RNA-2 and the mutant or wt RNA-3 were performed as described previously (36), with the following modifications. Approximately 300,000 protoplasts, transfected with a given mixture of viral transcripts, were separated into two equal batches. One aliquot was processed for Northern blot analysis as described above; the second was resuspended in Laemmli buffer with SDS and heated to 100°C. Equal sample volumes were loaded onto a SDS–12% polyacrylamide gel for electrophoresis and subsequent Western blot analysis.

RESULTS

A series of BMV RNA-3 deletion mutants that lacked sequences corresponding to single or multiple stem-loop structures predicted to be present in the 3'-NTR was constructed (Fig. 1). These RNA-3 deletion mutants were coinoculated with RNA-1 and -2 into barley protoplasts, and the effects of the deletions on viral replication were determined. RNA stability was assayed in vivo by using barley protoplasts, and mRNA functionality was examined by translation in vitro and in protoplasts. RNA-3 was chosen as a target for these mutations because the proteins that it encodes are not essential for replication, and their effects could be observed without fear of completely debilitating viral replication. Nevertheless, because progeny levels of BMV RNA positive and negative strands are greatly affected by the presence of a functional RNA-3, any debilitation of its replication was expected to alter strand asymmetry (36) as well as to yield profound effects on total progeny production.

Effect of deleting single or multiple stem-loop sequences on replication in barley protoplasts. When coinoculated with wt RNA-1 and -2, the replication of RNA-3 mutants bearing deletions of single structures H and K was not greatly reduced, RNA-3 progeny levels for both positive and nega-

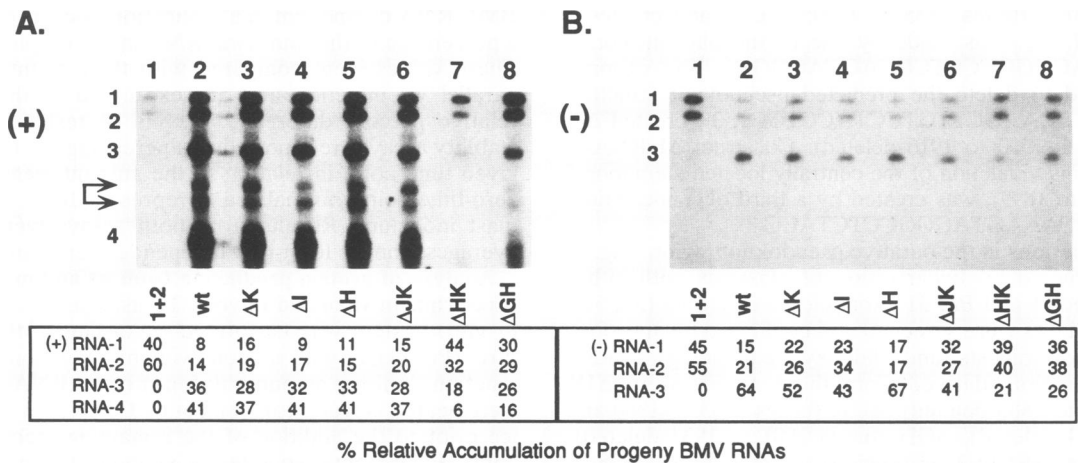

FIG. 2. Northern blot analysis of viral RNAs from barley protoplasts transfected with RNA-3 mutants bearing sequence deletions corresponding to single or double stem-loop deletions. Inocula contained transcripts of RNA-1 and -2 plus no RNA-3 (lanes 1), wt RNA-3 (lanes 2), ΔK RNA-3 (lanes 3), ΔI RNA-3 (lanes 4), ΔH RNA-3 (lanes 5), ΔJK RNA-3 (lanes 6), ΔHK RNA-3 (lanes 7), or ΔGH RNA-3 (lanes 8). Panels A and B show positive- and negative-strand progeny, respectively. Positions of BMV RNA-1, -2, -3, and -4 are shown to the left of each panel. Relative accumulations of individual progeny RNAs are tabulated as a percentage of the total RNA present in each lane. Because the values listed are averages of at least three independent experiments, their sum does not precisely equal 100%. The autoradiograph in panel B was exposed seven times longer than that in panel A. Arrows in panel A indicate the positions of viral RNA degradation products.

tive strands being not less than 78% of the wt level (Fig. 2, lanes 3 and 5). Although a 33% reduction in negative-strand progeny, relative to the wt counterpart, was recorded for the ΔI mutant, positive-strand accumulation was close to the wt level (Fig. 2, lanes 4). These observations imply a debilitation of the negative-strand promoter of RNA-3 and continued wt levels of positive-strand synthesis from available negative-strand templates; the latter finding supports hypotheses concerning the conversion of the negative-strand replicase to one dedicated to positive-strand synthesis (45). Inspection of the negative-strand progeny for the experiments shown in Fig. 2 reveals that relative increases in RNA-1 and -2 levels typically accompany a decrease in the level of RNA-3. It is likely that these increases yield high levels of positive-strand RNA-1 and -2 early in infection, resulting in enhanced amounts of viral replicase proteins p1 and p2 and very effective positive-strand replication (44). These observations are in accord with results from a recent study on the interactions of BMV RNA-1, RNA-2, and RNA-3 (13); even greater relative increases in negative-strand progeny for RNA-1 and RNA-2 were seen for transfections containing RNA-3 mutants bearing additional sequence deletions (see below).

Both positive- and negative-strand progeny from transfections containing RNA-3 mutants bearing deletions of sequences corresponding to two predicted pseudoknot structures (ΔJK, ΔHK, and ΔGH RNA-3) were decreased from wt levels (Fig. 2, lanes 6 to 8). Interestingly, although deletions ΔH and ΔK were not dramatically debilitated in replication, the ΔHK combination gave greatly reduced progeny levels relative to both RNA-3 (positive strand, 48%, and negative strand, 33% of the wt level) and RNA-4 (14% of the wt level; Fig. 2A, lane 7). The deletion of sequences corresponding to both structures J and K, on the other hand, gave a pattern of accumulation similar to that of a ΔK transfection (Fig. 2, lanes 6). Transfections including the ΔGH RNA-3 mutant resulted in an asymmetric positive-/negative-strand ratio of 57:1, compared with the >100:1 ratio typically found for wt infections (36). Since the intercistronic region of RNA-3 was previously seen to be a major determinant in controlling the positive-/negative-strand ratio (36), the effect of the downstream region is striking.

In general, progeny levels resulting from transfections with inocula containing RNA-3 mutants bearing extensive deletions in the putative pseudoknot region were very low (Fig. 3). However, transfections containing deletion mutants ΔGHI RNA-3 and ΔGHIJ RNA-3 (Fig. 3, lanes 2 and 3) yielded 69 and 54%, respectively, of wt positive-strand RNA-3 accumulation levels. Given that these deletions do not directly affect the subgenomic promoter present on RNA-3 (34, 35), the drastic crippling of RNA-4 production (to 6 and 12% of the wt level, respectively) in transfections containing these mutations is remarkable.

As seen in Fig. 3B, negative-strand RNA-1 and -2 progeny levels increased relative to a wt infection as the accumulation of negative-strand RNA-3 decreased. These increases were substantially greater than those seen for the single and double structure deletion mutants (Fig. 2B) and provide additional evidence for a reduction in competition for replicase by the strong negative-strand promoter present on RNA-3 with the negative-strand promoters on RNA-1 and RNA-2 that occurs in such situations (13). In the most extreme case tested, i.e., in transfections containing the ΔPsKs RNA-3 mutant, only RNA-1 and RNA-2 replicated (Fig. 3, lanes 6). The accumulation levels of RNA-1 and RNA-2 from such transfections were very similar to those resulting from transfections with RNA-1 plus RNA-2 in the absence of RNA-3 (Fig. 3, lanes 6 and 7). A similar pattern of progeny accumulation was observed (data not shown) for transfections including RNA-3 mutant 1984/BΔt, in which the tRNA-like structure downstream of position 2026 is deleted (Fig. 1A).

Stability of input RNA-3 transcripts in barley protoplasts. To examine the effects of 3′-end deletions on RNA stability, the half-lives ($t_{1/2}$) of selected RNA-3 mutants were determined in protoplasts (Fig. 4). Deletion of the tRNA-like structure (mutant 1984/BΔt) had little effect on stability ($t_{1/2}$ of approximately 3 h) compared with the wild-type sequence

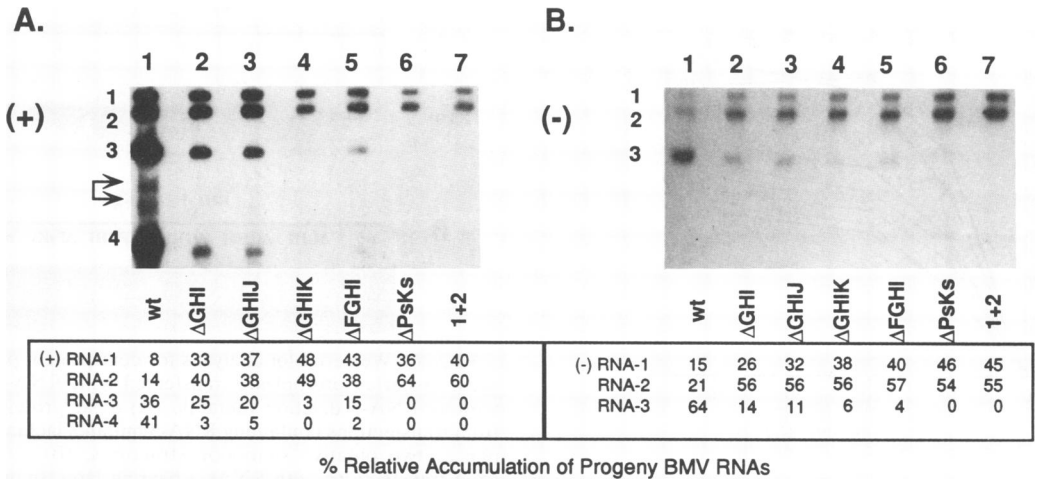

	wt	ΔGHI	ΔGHIJ	ΔGHIK	ΔFGHI	ΔPsKs	1+2
(+) RNA-1	8	33	37	48	43	36	40
RNA-2	14	40	38	49	38	64	60
RNA-3	36	25	20	3	15	0	0
RNA-4	41	3	5	0	2	0	0

	wt	ΔGHI	ΔGHIJ	ΔGHIK	ΔFGHI	ΔPsKs	1+2
(-) RNA-1	15	26	32	38	40	46	45
RNA-2	21	56	56	56	57	54	55
RNA-3	64	14	11	6	4	0	0

FIG. 3. Northern blot analysis of viral RNAs from protoplasts transfected with RNA-3 mutants bearing large sequence deletions in the 3′-NTR. Inocula contained transcripts of RNA-1 and -2 plus wt RNA-3 (lanes 1), ΔGHI RNA-3 (lanes 2), ΔGHIJ RNA-3 (lanes 3), ΔGHIK RNA-3 (lanes 4), ΔFGHI RNA-3 (lanes 5), ΔPsKs RNA-3 (lanes 6), or no RNA-3 (lanes 7). Panels A and B show positive- and negative-strand progeny, respectively. Relative accumulations of individual progeny RNAs are tabulated as a percentage of the total RNA present in each lane and are averages of at least two independent experiments. The autoradiograph in panel B was exposed eight times longer than the one in panel A.

($t_{1/2}$ of 3.7 h). The half-life of ΔPsKs RNA-3, however, was about 2 h shorter than that of wt RNA-3 for the first 3 h postinoculation. In three independent experiments, this 3-h value for ΔPsKs RNA-3 was the only time point at which the stability kinetics of the mutant RNAs consistently differed from those of wt RNA-3. This finding indicates that these 3′ distal sequences (possibly in conjunction with predicted secondary structures) positively influence the stability of viral RNA, while deletion of the tRNA-like structure has a neutral effect on the half-life of the message.

Effect of 3′ sequence deletions on translatability in vitro. To evaluate whether this region exerts translational control on BMV RNA-3, whose first open reading frame encodes the proposed movement protein, p3 (4), transcripts of wt or deletion mutant RNA-3 were translated in vitro. Comparison of the amount of labeled peptide product indicated few differences between the mutant and wt sequences. The translation of mutant RNAs lacking one or two putative structures yielded higher levels of [^{35}S]methionine incorporation than were obtained for wt RNA (Fig. 5A), as did the mutant (Fig. 5B, ΔPsKs) lacking most of this region. The mutant RNAs bearing larger deletions directed 70 to 80% of wt incorporation levels (Fig. 5B). Translation of the 1984/BΔt template also paralleled wt activities (data not shown). No significant difference in the kinetics of translation was observed between wt RNA and the various mutant RNAs (data not shown). These data indicate that no important relationship exists for BMV RNA-3 between the presence of this putatively structured 3′ region and message translatability.

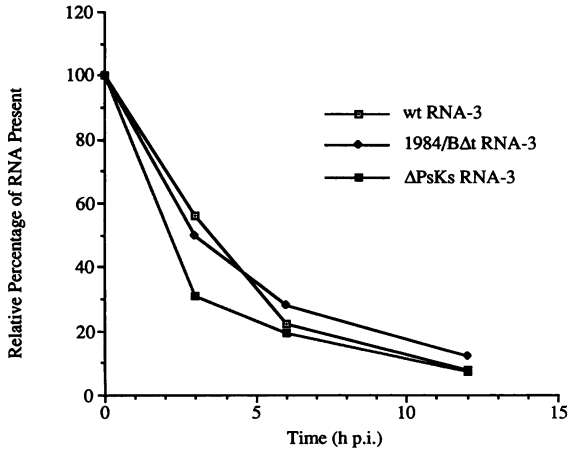

FIG. 4. Stability of viral RNA transcripts in barley protoplasts. Barley protoplasts were transfected with wt RNA-3, 1984/BΔt RNA-3, or ΔPsKs RNA-3 transcripts (3 μg of each). RNA was extracted from protoplasts harvested at 0, 3, 6, or 12 h. RNA accumulation was determined by densitometry of RNA blots, and the values for each time point (averages of three independent experiments) expressed as a percentage of the level present at 0 h postinoculation (p.i.).

Coat protein accumulation directed by mutant RNAs in vivo. To further determine the effects of sequence deletions on the translatability of these messages, we undertook Western blot analysis of coat protein produced in protoplasts transfected with inocula including the various mutants. The cells were divided into equal samples for use in Northern and Western blot analyses to directly compare amounts of RNA-4 and coat protein produced. Because RNA-4 derives its 3′-NTR from the negative-strand RNA-3 template, any sequence deletion of the 3′ end would be conserved in this message. As seen in Fig. 6, the amount of coat protein detected resembled the observed production of positive-strand RNA-4 derived from the mutant RNA-3 templates (Fig. 2 and 3 and data not shown). This finding indicates that while the deletions do not affect translatability per se, they exert an effect on coat protein production through modulating the level of RNA-4 synthesis.

DISCUSSION

In common with other aminoacylatable, nonpolyadenylated RNA viruses, the 3′-NTR of BMV RNAs exhibits several functional features. These are related to tRNA-like

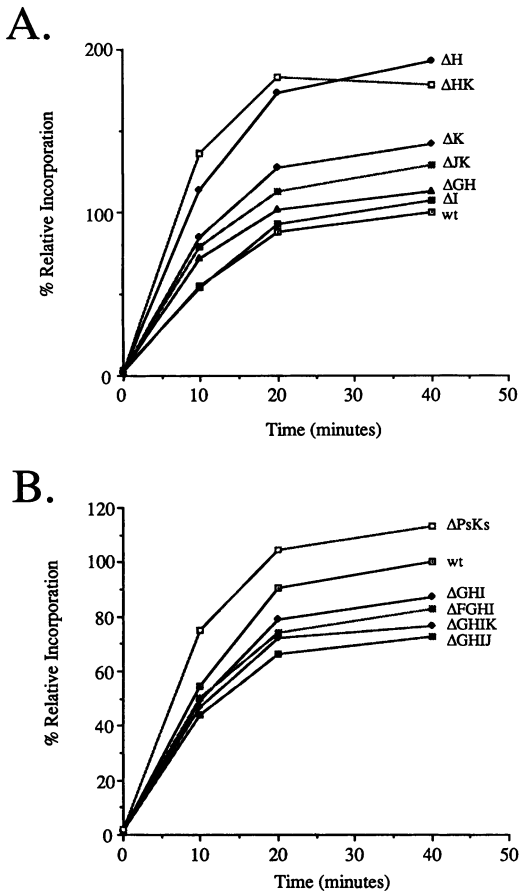

FIG. 5. Translatability of wt and RNA-3 deletion mutants. Deletion mutation RNA-3 were used as mRNAs to direct the production of protein in an in vitro wheat germ translation system. Product was measured by determining the percent incorporation of [^{35}S]methionine into trichloroacetic acid-precipitable protein. Values expressed are relative to the percent incorporation obtained with wt RNA-3 template after incubation for 40 min. (A) Messenger activity of RNA-3 deletion mutants lacking to one or two putative structures; (B) messenger activity of RNA-3 mutants bearing multiple deletions in the 3′-NTR. Results are averages of at least three independent experiments; note the difference in scale for panels A and B.

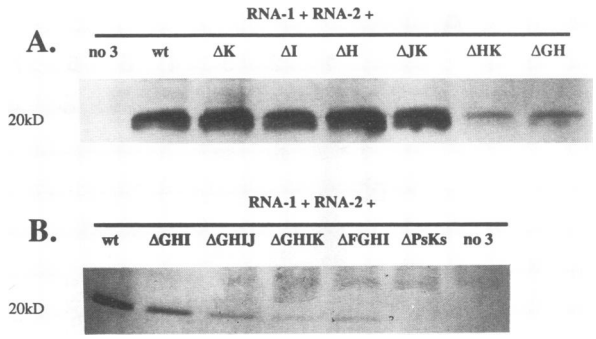

FIG. 6. Western blot analyses for coat protein products synthesized in barley protoplasts transfected with RNA-1, RNA-2, and various RNA-3 deletion mutants. (A) Coat protein accumulation from transfections containing RNA-3 mutants lacking sequences for one or two putative stem-loop structures; (B) products detected from transfections with RNAs-3 bearing large sequence deletions. No coat protein was produced from transfections containing only RNA-1 and -2 (lanes designated "no 3").

structures and their ability to utilize host tRNA-associated enzymes, such as aminoacyl-tRNA synthetases and nucleotidyltransferases (22, 23). Sequences upstream of these tRNA-like structures remain largely uncharacterized as to their role(s) in viral function (41). Whereas deletion of the 3′ proximal pseudoknot sequence in TMV RNA prevents replication in protoplasts (56), no such drastic effect resulted upon elimination of an individual stem-loop structure from BMV RNA-3. However, deletion of sequences containing stem-loop K yielded RNAs with reduced ability to replicate (78% of wt levels; Fig. 2), the effect being more marked than for constructs bearing deletions of similar lengths that did not contain this sequence.

Deletions of putative secondary structures decrease genomic negative-strand and subgenomic positive-strand accumulation. In transfections containing RNA-3 deletion mutants, the accumulation of negative-strand RNA was lower than that of the complementary positive-strand progeny compared with a wt infection. When ΔGHI RNA-3 was transfected into protoplasts, only 23% of negative-strand progeny, relative to wt levels of RNA-3, were detected (Fig. 3B, lane 2), suggesting that the negative-strand promoter in the tRNA-like structure was weakened. This selective reduction in negative-strand synthesis may be explained by either of two hypotheses. First, this region may contain additional sequence or structural elements for complete negative-strand promotion. Second, these upstream structures of the 3′-NTR may provide the spatial context for the correct assembly and initiation of the replicase complex. The latter view is supported by an in vitro analysis of these RNAs as templates for complementary strand synthesis utilizing isolated replicase preparations (31).

The large sequence deletions (Fig. 3) are relatively distant from both the 3′ negative-strand promoter and the intercistronic subgenomic positive-strand promoter. However, even though the negative-strand ΔGHI RNA-3 template was still functional, allowing the generation of 69% of wt amounts of positive-strand RNA-3 progeny, low amounts (<10% of the wt level) of positive-strand subgenomic RNA-4 were produced. Consequently, this observed decrease in positive-strand RNA-4 progeny from negative-strand RNA-3 templates derived from these mutants provides evidence that the regions deleted normally interact with upstream elements. An alternative explanation for low levels of subgenomic RNA production is that when very low levels of negative-strand RNA-3 are present, they are dedicated to the production of positive-strand genomic RNA-3; i.e., production of RNA-4 occurs only when an adequate supply of negative-strand RNA-3 is available. Indeed, the data shown in Fig. 3 indicate that at least 15% of wt levels of negative-strand RNA-3 is required for production of subgenomic RNA-4. Mutant ΔHK RNA-3 yielded 33% of wt levels of negative-strand RNA-3 and 15% of wt levels of the subgenomic RNA-4 message (Fig. 2, lanes 7); such levels may approach the minimum requirement for systemic spread in plants as noted previously (12) for the pseudoknot mutant 5′PsK (within the 3′ tRNA-like structure), which produced 20% of wt RNA-3 levels in protoplasts and was barely successful in establishing a systemic infection in barley.

Deletions in the 3′-NTR alter positive-/negative-strand progeny ratios. Whereas the ratio for BMV RNA positive-/

negative-strand progeny exceeds 100:1 in the presence of wt RNA-3, this ratio is near parity in its absence (36). A major determinant for the difference was shown to be interactions involving the intercistronic region of RNA-3. A comparison of the positive- and negative-strand progeny levels shown in Fig. 2 and 3 reveals that in general, deletions involving multiple predicted structures yield lower positive-/negative-strand ratios than do those with shorter sequence deletions. For example, transfections involving mutant ΔGH RNA-3 produced RNA-3 progeny positive strands that were 72% of wt and negative strands that were 41% of wt (Fig. 2, lanes 8), yielding a positive-/negative-strand ratio of 57:1. A similar comparison for the large sequence deletion mutants (Fig. 3) yielded ratios ranging from 32:1 (ΔGHI RNA-3) to 1:1 (ΔGHIK RNA-3). These observations indicate decreased negative-strand promotion for the RNA-3 mutants. They also provide additional evidence for the existence of interactions between the structures in 3′-NTR and upstream sequence elements, especially the intercistronic region, these interactions being impaired by the deletions. Alternatively, the effect observed may be due to the low levels of negative-strand RNA-3 produced from these mutant templates, as discussed above for the low production of subgenomic RNA. In any case, such decreases undoubtedly contribute to lowered levels of RNA-3 progeny and reduce efficacy in systemic infection.

The reductions in RNA-3 accumulation observed may be due to two influences. First, the optimal folding of a particular mutant sequence may differ considerably from that predicted. In two recent computer programs effective in predicting pseudoknots (1, 21), the algorithms are written to assume that RNA folds in a stepwise, nearest-neighbor manner. Therefore, the manner in which a mutant RNA folds as it is being synthesized may potentially yield several alternative secondary structures in the 3′-NTR that are distinct from the predicted folding of the native form. Evidence from our analyses (31) of these templates for complementary strand synthesis in vitro, however, suggests that the minimal negative-strand promoter sequences in the downstream tRNA-like structure do retain a functional configuration, despite deletions present upstream. Second, the predicted positions of various pseudoknots and stem-loops may provide localized stability in the 3′-NTR. In this way, the loss of structures K and J is not as debilitating as the loss of both structures K and H (Fig. 2, lanes 6 and 7), which are separate sequences and structures in terms of location. The possibility that the local sequence environment affects viral functions through its effect on RNA folding was proposed (56) to explain the high level (90%) of progeny accumulation observed in protoplasts for a TMV pseudoknot deletion mutant (S-6253) that was defective in systemic spread.

The results reported here do not directly differentiate between effects caused by indispensable sequence or structure elements. However, they are in accord with the concept that upstream sequences of the 3′-NTR correctly present the downstream tRNA-like structure to the viral replicase complex. The importance of the sequence context to the overall functionality of a given promoter has been established by using exchanges of the highly conserved 3′ termini (that include part of the extended upstream region studied here) among BMV genomic RNAs (13). Requirements for RNA secondary structure and space for proper presentation of 3′-terminal sequence elements involved in polyadenylation have also been noted in both viral (27) and cellular (6) systems.

Role of the putative pseudoknot region in RNA stability. The correlation between an increased RNA half-life and the formation of a poly(A)-poly(A)-binding protein complex has been reviewed by Bernstein and Ross (5). Stem-loop structures found in the 3′ region of plastid and histone mRNAs have been shown to create stable terminal sequences (2, 39, 53). Gallie and Walbot (19) found that the $t_{1/2}$ of a chimeric GUS-TMV 3′-NTR transcript was similar to that of a message bearing a poly(A) tail. Subsequently, it was reported (17) that the tRNA-like structure alone makes the greatest contribution to the chimeric GUS message's stability. In the natural context of BMV RNA, however, this does not seem to be the case. Our results show that while ΔPsKs RNA-3 has a $t_{1/2}$ 2 h shorter than the wt $t_{1/2}$ in the first 3 h postinoculation in protoplasts, deletion of the tRNA-like structure does not significantly lower the stability of the transcript (Fig. 4). Discrepancies between our results, based on tests with viral cDNA transcripts, and those from the GUS-TMV chimera work may be due to differences in the higher-order structures of the two molecules. This idea is reinforced by the observation that RNA-3 molecules are characterized by a $t_{1/2}$ of >3 h, considerably longer than the $t_{1/2}$ of 70 to 90 min (17) for the chimeric RNAs. Indeed, Gallie et al. (18) reported that the translation and stability of a chimeric message can be highly reporter gene dependent, suggesting that defined elements of a complete mRNA contribute to the utilization of that message. These results suggest that caution should be used when one compares the functionality of a particular RNA sequence in native and chimeric contexts.

Deletions in the 3′-NTR do not necessarily decrease translatability. The 3′-NTRs of polyadenylated RNAs can either positively (9, 20, 26) or negatively (30) affect protein translation from the mRNA template. The presence of the 3′-NTR of TMV RNA was found to enhance translation of a GUS reporter gene in vivo (19), the sequence including three pseudoknots playing the major role in this effect (17). However, we found that while deletion of sequences for several putative structures in this region of BMV RNA-3 was slightly detrimental to translation kinetics and accumulation of p3 in vitro (Fig. 5B), sequence deletions of one or two structures and even the entire region (ΔPsKs) could enhance translation (Fig. 5A and B).

The differential effects found here for individual deletions within the 3′ terminus of BMV RNA-3 suggest that it may be unwise to extrapolate effects on translation from one or even a limited series of constructs. It is important to consider the possibility that in vitro systems do not reflect differences in mRNA translatability that are seen in vivo (9, 16). However, our results, derived from the translation of mRNAs of a virus infecting monocots in a monocot (wheat germ) system, show mutant mRNA activities that are well above and below wt levels, suggesting that the in vitro translation system used can distinguish functional differences. Importantly, host cell-native viral RNA interactions may confer regulatory properties (such as subcellular location) that cannot be approximated by a reporter system. The role of genomic secondary structure in the temporal control of gene expression in phage RNA is well known (14), and the sequence complementarity between the 5′ and 3′ ends of the aminoacylatable plant viral RNAs BMV RNA-3 (8), TYMV RNA (15), and TMV RNA (15) can obscure the start codon of the first open reading frame. This observation suggests that these viral mRNAs exist in several distinct forms, some of which cannot be translated. Experimental evidence showing that TYMV RNA can form circular structures in solution (55) and that neither BMV RNA-3 nor -4 gives rise to

detectable protein products when inoculated alone into barley protoplasts (7, 29) provides support to this concept.

The effects of deletions in the 3′-NTR on replication transcend their effects on translation. While Fig. 5 shows that the translatability of p3 from RNA-3 bearing the ΔPsKs mutation exceeded that of wt RNA-3 in vitro, translation of coat protein from RNA-4 template bearing this mutation in vitro was also found to be slightly better than that from wt RNA-4 (7). Additionally, the accumulation of coat protein in protoplasts (Fig. 6) closely followed the observed levels of RNA-4 template (Fig. 2 and 3 and data not shown). These findings show that although little, if any, coat protein was detected for the ΔPsKs mutant in protoplasts, this reflects the debilitation of subgenomic RNA-4 production rather than its translatability.

Conclusions. The different lengths and predicted structural configurations of the BMV RNA-1, -2, and -3 stem-loop regions (42, 43) may contribute significantly to the optimal genomic context for the negative-strand promoter activities of these RNAs (13). The predicted ability of these sequences to collectively form a quasi-double-stranded RNA stalk that stably presents the tRNA-like structure to BMV replicase and associated proteins could represent the basis for these optimal intragenic interactions. This concept is in accord with our observations that, in general, deletions within this region decrease replication efficacy, decrease the proportion of negative-strand RNA-3 progeny, and lower strand asymmetry.

ACKNOWLEDGMENTS

We thank Rohit Duggal, Clayton Huntley, Greg Pogue, and A. L. N. Rao for helpful discussions and critical review of the manuscript, Jim Connell and Naomi Trevino for technical assistance, and W. David Worrall, TAES-Vernon, for supplying barley (*H. vulgare* cv. Dickson) seeds.

These studies were supported by NSF grant DMB-8921023.

REFERENCES

1. **Abrahams, J. P., M. van den Berg, E. van Batenburg, and C. Pleij.** 1990. Prediction of RNA secondary structure, including pseudoknotting, by computer simulation. Nucleic Acids Res. **18:**3035–3044.
2. **Adams, C. C., and D. B. Stern.** 1990. Control of mRNA stability in chloroplasts by 3′ inverted repeats: effects of stem and loop mutations on degradation of *psb*A mRNA in vitro. Nucleic Acids Res. **18:**6003–6010.
3. **Ahlquist, P., R. Dasgupta, and P. Kaesberg.** 1981. Near identity of 3′ RNA secondary structure in bromoviruses and cucumber mosaic virus. Cell **23:**183–189.
4. **Allison, R., C. Thompson, and P. Ahlquist.** 1990. Regeneration of a functional RNA virus genome by recombination between deletion mutants and requirement for cowpea chlorotic mottle virus 3a and coat genes for systemic infection. Proc. Natl. Acad. Sci. USA **87:**1820–1824.
5. **Bernstein, P., and J. Ross.** 1989. Poly(A), poly(A) binding protein and the regulation of mRNA stability. Trends Biochem. Sci. **14:**373–377.
6. **Brown, P. H., L. S. Tiley, and B. R. Cullen.** 1991. Effect of RNA secondary structure on polyadenylation site selection. Genes Dev. **5:**1277–1284.
7. **Connell, J. P., and T. C. Hall.** 1992. Unpublished data.
8. **Dasgupta, R., P. Ahlquist, and P. Kaesberg.** 1980. Sequence of the 3′ untranslated region of brome mosaic virus coat protein messenger RNA. Virology **104:**339–346.
9. **Doel, M. T., and N. H. Carey.** 1976. The translational capacity of deadenylated ovalbumin messenger RNA. Cell **8:**51–58.
10. **Dreher, T. W., and T. C. Hall.** 1988. Mutational analysis of the sequence and structural requirements in brome mosaic virus RNA for minus strand promoter activity. J. Mol. Biol. **201:**31–40.
11. **Dreher, T. W., and T. C. Hall.** 1988. Mutational analysis of the tRNA mimicry of brome mosaic virus RNA: sequence and structural requirements for aminoacylation and 3′-adenylation. J. Mol. Biol. **201:**41–55.
12. **Dreher, T. W., A. L. N. Rao, and T. C. Hall.** 1989. Replication in vivo of mutant brome mosaic virus RNAs defective in aminoacylation. J. Mol. Biol. **206:**425–438.
13. **Duggal, R., A. L. N. Rao, and T. C. Hall.** 1992. Unique nucleotide differences in the conserved 3′ termini of brome mosaic virus RNAs are maintained through their optimization of genome replication. Virology **187:**261–270.
14. **Fiers, W.** 1979. Structure and function of RNA bacteriophages, p. 69–204. *In* H. Frankel-Conrat and R. R. Wagner (ed.), Comprehensive virology, vol. 13. Plenum Press, New York.
15. **Florentz, C., J. P. Briand, and R. Giegé.** 1984. Possible functional role of viral tRNA-like structures. FEBS Lett. **176:**295–300.
16. **Gallie, D. R.** 1991. The cap and poly(A) tail function synergistically to regulate mRNA translational efficiency. Genes Dev. **5:**2108–2116.
17. **Gallie, D. R., J. N. Feder, R. T. Schimke, and V. Walbot.** 1991. Functional analysis of the tobacco mosaic virus tRNA-like structure in cytoplasmic gene regulation. Nucleic Acids Res. **19:**5031–5036.
18. **Gallie, D. R., J. N. Feder, R. T. Schimke, and V. Walbot.** 1991. Post-transcriptional regulation in higher eukaryotes: the role of the reporter gene in controlling expression. Mol. Gen. Genet. **228:**258–264.
19. **Gallie, D. R., and V. Walbot.** 1990. RNA pseudoknot domain of tobacco mosaic virus can functionally substitute for a poly(A) tail in plant and animal cells. Genes Dev. **4:**1149–1157.
20. **Grens, A., and I. E. Scheffler.** 1990. The 5′- and 3′-nontranslated regions of ornithine decarboxylase mRNA affect the translational efficiency. J. Biol. Chem. **265:**11810–11816.
21. **Gultyaev, A. P.** 1991. The computer simulation of RNA folding involving pseudoknot formation. Nucleic Acids Res. **19:**2489–2494.
22. **Hall, T. C.** 1979. Transfer RNA-like structures in viral genomes. Int. Rev. Cytol. **60:**1–26.
23. **Hall, T. C., L. E. Marsh, and T. W. Dreher.** 1987. Analysis of brome mosaic virus replication and aminoacylation functions by site-specific mutagenesis. J. Cell Sci. Suppl. **7:**287–301.
24. **Hall, T. C., D. S. Shih, and P. Kaesberg.** 1972. Enzyme-mediated binding of tyrosine to brome-mosaic-virus-ribonucleic acid. Biochem. J. **129:**969–976.
25. **Hatfield, D., and S. Oroszlan.** 1990. The *where*, *what* and *how* of ribosomal frameshifting in retroviral protein synthesis. Trends Biochem. Sci. **15:**186–190.
26. **Ingelbrecht, I. L. W., L. M. F. Herman, R. A. Dekeyser, M. C. Van Montagu, and A. G. Depicker.** 1989. Different 3′ end regions strongly influence the level of gene expression in plant cells. Plant Cell **1:**671–680.
27. **Iwasaki, K., and H. M. Temin.** 1990. The efficiency of RNA 3′ end formation is determined by the distance between the cap site and the poly(A) site in spleen necrosis virus. Genes Dev. **4:**2299–2307.
28. **Joshi, R. L., S. Joshi, F. Chapeville, and A. L. Haenni.** 1983. tRNA-like structures of plant viral RNAs: conformational requirements for adenylation and aminoacylation. EMBO J. **2:**1123–1127.
29. **Kiberstis, P. A., L. S. Loesch-Fries, and T. C. Hall.** 1981. Viral protein synthesis in barley protoplasts inoculated with native and fractionated brome mosaic virus RNA. Virology **112:**804–808.
30. **Kruys, V., M. Wathelet, P. Poupart, R. Contreras, W. Fiers, J. Content, and G. Huez.** 1987. The 3′ nontranslated region of the human interferon-β mRNA has an inhibitory effect on translation. Proc. Natl. Acad. Sci. USA **84:**6030–6034.
31. **Lahser, F. C., and T. C. Hall.** Unpublished data.
32. **Laskey, R. A., and A. D. Mills.** 1977. Enhanced autoradiographic detection of ^{32}P and ^{125}I using intensifying screens and hypersensitized film. FEBS Lett. **82:**314–316.
33. **Loesch-Fries, L. S., and T. C. Hall.** 1980. Synthesis, accumula-

tion and encapsidation of individual brome mosaic virus RNA components in barley protoplasts. J. Gen. Virol. **47**:323–332.
34. **Marsh, L. E., T. W. Dreher, and T. C. Hall.** 1987. Mutational analysis of the internal promoter for transcription of subgenomic RNA4 of BMV, p. 327–336. *In* M. Brinton and R. Rueckert (ed.), Positive strand RNA viruses. Alan R. Liss, Inc., New York.
35. **Marsh, L. E., T. W. Dreher, and T. C. Hall.** 1988. Mutational analysis of the core and modulator sequences of the BMV RNA3 subgenomic promoter. Nucleic Acids Res. **16**:981–995.
36. **Marsh, L. E., C. C. Huntley, G. P. Pogue, J. P. Connell, and T. C. Hall.** 1991. Regulation of (+):(−)-strand asymmetry in replication of brome mosaic virus RNA. Virology **182**:76–83.
37. **McLeester, R. C., and T. C. Hall.** 1977. Simplification of amino acid incorporation and other assays using filter paper techniques. Anal. Biochem. **79**:627–630.
38. **Miller, W. A., J. J. Bujarski, T. W. Dreher, and T. C. Hall.** 1986. Minus-strand initiation by brome mosaic virus replicase within the 3′ tRNA-like structure of native and modified RNA templates. J. Mol. Biol. **187**:537–546.
39. **Pandy, N. B., and W. F. Marzluff.** 1987. The stem-loop structure at the 3′ end of histone mRNA is necessary and sufficient for regulation of histone mRNA stability. Mol. Cell. Biol. **7**:4557–4559.
40. **Perret, V., C. Florentz, T. W. Dreher, and R. Giegé.** 1989. Structural analogies between the 3′ tRNA-like structure of brome mosaic virus RNA and yeast $tRNA^{Tyr}$ revealed by protection studies with yeast tyrosyl-tRNA synthetase. Eur. J. Biochem. **185**:331–339.
41. **Pleij, C. W. A.** 1990. Pseudoknots: a new motif in the RNA game. Trends Biochem. Sci. **15**:143–147.
42. **Pleij, C. W. A.** 1992. Personal communication.
43. **Pleij, C. W. A., J. P. Abrahams, A. Van Belkum, K. Rietveld, and L. Bosch.** 1987. The spatial folding of the 3′ noncoding region of aminoacylatable plant viral RNAs, p. 299–316. *In* M. Brinton and R. Rueckert (ed.), Positive strand RNA viruses. Alan R. Liss, Inc., New York.
44. **Pogue, G. P., and T. C. Hall.** 1992. The requirement for a 5′ stem-loop structure in brome mosaic virus replication supports a new model for viral positive-strand RNA initiation. J. Virol. **66**:674–684.
45. **Pogue, G. P., L. E. Marsh, J. P. Connell, and T. C. Hall.** 1992. Requirement for ICR-like sequences in the replication of brome mosaic virus genomic RNA. Virology **188**:742–753.
46. **Pogue, G. P., L. E. Marsh, and T. C. Hall.** 1990. Point mutations in the ICR2 motif of brome mosaic virus RNAs debilitate (+)-strand replication. Virology **178**:152–160.
47. **Rao, A. L. N., T. W. Dreher, L. E. Marsh, and T. C. Hall.** 1989. Telomeric function of the tRNA-like structure of brome mosaic virus RNA. Proc. Natl. Acad. Sci. USA **86**:5335–5339.
48. **Rietveld, K., K. Linschooten, C. W. A. Pleij, and L. Bosch.** 1984. The three-dimensional folding of the tRNA-like structure of tobacco mosaic virus RNA. A new building principle applied twice. EMBO J. **3**:2613–2619.
49. **Rietveld, K., C. W. A. Pleij, and L. Bosch.** 1983. Three dimensional models of the tRNA-like termini of some plant viral RNAs. EMBO J. **2**:1079–1085.
50. **Rietveld, K., R. Van Poelgeest, C. W. A. Pleij, J. H. Van Boom, and L. Bosch.** 1982. The tRNA-like structure at the 3′ terminus of turnip yellow mosaic virus RNA. Differences and similarities with canonical tRNA. Nucleic Acids Res. **10**:1929–1946.
51. **Sambrook, J., E. F. Fritsch, and T. Maniatis.** 1989. Molecular cloning: a laboratory manual. Cold Spring Harbor Laboratory Press, Cold Spring Harbor, N.Y.
52. **Schimmel, P.** 1989. RNA pseudoknots that interact with components of the translation apparatus. Cell **58**:9–12.
53. **Stern, D. B., E. R. Radwanski, and K. L. Kindle.** 1991. A 3′ stem/loop structure of the *Chlamydomonas* chloroplast *atpB* gene regulates mRNA accumulation in vivo. Plant Cell **3**:285–297.
54. **Stern, S., B. Weiser, and H. F. Noller.** 1988. Model for the three-dimensional folding of 16 S ribosomal RNA. J. Mol. Biol. **204**:447–481.
55. **Strazielle, C., H. Benoit, and L. Hirth.** 1965. Particularités structurales de l'acide ribonucléique extrait du virus de la mosaique jaune du navet. II. J. Mol. Biol. **13**:735–748.
56. **Takamatsu, N., Y. Watanabe, T. Meshi, and Y. Okada.** 1990. Mutational analysis of the pseudoknot region in the 3′ noncoding region of tobacco mosaic virus RNA. J. Virol. **64**:3686–3693.
57. **Tang, C. K., and D. E. Draper.** 1989. Unusual mRNA pseudoknot structure is recognized by a protein translational repressor. Cell **57**:531–536.
58. **Ten Dam, E. B., C. W. A. Pleij, and L. Bosch.** 1990. RNA pseudoknots: translational frameshifting and readthrough on viral RNAs. Virus Genes **4**:121–136.
59. **Van Belkum, A., J. P. Abrahams, C. W. A. Pleij, and L. Bosch.** 1985. Five pseudoknots are present at the 204 nucleotides long 3′ noncoding region of tobacco mosaic virus RNA. Nucleic Acids Res. **13**:7673–7686.